DesignCon 2009

Measurement-Assisted Electromagnetic Extraction of Interconnect Parameters on Low-Cost FR-4 boards for 6-20 Gb/sec Applications

Yuriy Shlepnev, Simberian Inc.
shlepnev@simberian.com, +1-206-409-2368

Alfred Neves, Teraspeed Consulting Group
al@teraspeed.com, + 1-503-718-7172

Tom Dagostino, Teraspeed Consulting Group
tom@teraspeed.com, +1-503-430-1065

Scott McMorrow, Teraspeed Consulting Group
scott@teraspeed.com, +1- (401) 284-1827

Abstract
Design of interconnects on PCBs for 6-10 Gb/s data rates requires electromagnetic models from DC up to 20 GHz. Manufacturers of low-cost FR-4 PCBs typically provide values for dielectric constant and loss tangent either at one frequency or without specifying frequency value at all, that is not acceptable for the broad-band models. A simple and practical methodology to extract frequency-dependent dielectric parameters on the base of correlation of measurements and simulations is proposed. A board with 30 test structures has been built to validate the extraction methodology and to verify possibilities to predict interconnect parameters with the electromagnetic analysis.

Authors Biographies
Yuriy Shlepnev is the president and founder of Simberian Inc., were he develops electromagnetic software for advanced analysis of interconnects. He received M.S. degree in radio engineering from Novosibirsk State Technical University in 1983, and the Ph.D. degree in computational electromagnetics from Siberian State University of Telecommunications and Informatics in 1990. He was principal developer of a planar 3D electromagnetic simulator for Eagleware Corporation. From 2000 to 2006 he was a principal engineer at Mentor Graphics Corporation, where he was leading the development of electromagnetic software for simulation of high-speed digital circuits. The results of his research are published in multiple papers and conference proceedings.

Alfred Neves is a Senior Staff Signal Integrity Engineer working with Teraspeed Consulting LLC. He received BSEE degree in Mathematics from University of Massachusetts. He has worked in the Signal integrity field for 13 years focusing on backplane design, advanced jitter analysis, practical metrology issues, and a host of other accomplishments.

Tom Dagostino is Vice President of Teraspeed Consulting Group. Tom Dagostino currently manages and models in the Teraspeed Consulting Group LLC's Device Characterization Division. Mr. Dagostino has over 14 years experience in Signal Integrity modeling, previously with Zeelan Technologies and Mentor Graphics. Prior assignments have included over 18 years with Tektronix program managing, designing and performing market research on Digital Storage Oscilloscopes, real time oscilloscopes, probes and technology. Mr. Dagostino holds 10 Patents relating to DSO technologies and product features.

Scott McMorrow is President and Founder of Teraspeed Consulting Group**.** Mr. McMorrow is an experienced technologist with over 20 years of broad background in complex system design, interconnect & Signal Integrity engineering, modeling & measurement methodology, engineering team building and professional training. Mr. McMorrow has a consistent history of delivering and managing technical consultation that enables clients to manufacture systems with state-of-the-art performance, enhanced design margins, lower cost, and reduced risk. Mr McMorrow is an expert in high-performance design and signal integrity engineering, and has been a consultant and trainer to engineering organizations world-wide.

1. Introduction

Interconnects of communication links with data rates 6-20 Gb/s require modeling over the frequency band from DC to at least 20 GHz validated with the measurements. Such models have to take into account conductor and dielectric loss and dispersion effects, full-wave nature of the fields in transmission lines and around the discontinuities. It is practically not possible to account for all those effects by tuning a static field solver, typically used in signal integrity software. Instead, 3D full-wave electromagnetic analysis has to be used to characterize interconnects at these data rates and the industry is currently in transition to the electromagnetic model based signal integrity analysis.

Unfortunately even 3D full-wave analysis may be not accurate if material properties are not well defined or approximated with narrow-band or non-causal models. Manufacturers of low-cost PCBs typically provide value of dielectric constant at one frequency or without specifying the frequency at all. It is important to establish a procedure to identify broadband dielectric properties for a particular manufacturing process before doing any board exploration with electromagnetic tools.

Multiple techniques for dielectric properties identification have been developed for planar microwave applications in 80-s and 90-s [1]-[5], [9] and recently for digital PCB and packaging applications [6]-[8], [10]-[15]. Analyses of different identification techniques are provided in [6], [7], [9], [13]. Capacitor structures are recommended by IPC standard for low frequencies and techniques based on strip-line or resonators are recommended for higher frequencies [6], [13].

All dielectric parameters identification techniques are based on correlation of measurements with a numerical model of the investigated structure. Practically all algorithms use VNA frequency-domain measurements of S-parameters. Though, TDR measurements are routinely used in PCB industry to identify dielectric properties by correlation with the results of a static field solver, but such simple approach is limited to relatively low frequencies and does not produce frequency-depend dielectric parameters. Researches from IBM suggested advanced technique based on TDR/TDT [8] that produces frequency-dependent parameters and appropriately separates conductor-related effects such as roughness. In [16] TDR is used at low frequencies in combination with VNA measurements at high frequencies to extract broad-band RLGC(f) models for multi-conductor lines (such models can be used to identify dielectric properties). On the numerical side, analytical formula-based or closed-form algorithms were originally used in microwave applications [1]-[5] and recently in digital applications [10], [15]. Commercial static or quasi-static solvers are used in [11], [14] and in PCB manufacturing industry in general. Commercial 3D full-wave software packages are used in [13], [9]. Some authors developed new algorithms to overcome the limitations of off-the-shelf software [8], [12].

Accuracy and limitations of a particular method can be characterized by accuracy of the measurement methodology and by sensitivity to measurement errors on one side and by approximations used in the computational model on the other side. Typical limitations of the electromagnetic models are absence of the broad-band

dielectric models, no roughness or oversimplified roughness models and only asymptotic conductor interior models in general.

Techniques based on **transmission line segments** [1], [4], [5], [7], [10], [11], [14], [15] are probably the most popular, but it is very sensitive to the de-embedding quality, repeatability and quality of the launches. Though the line segments are as close to interconnects on the board as it can get, connector or probe launches can degrade the accuracy the extracted dielectric parameters [4], [9].

Technique based on **patch resonators or cavities** excited directly with SMA connectors or probes as in [10], [12], [13], [15] are based on correlation of resonant frequencies that are relative insensitive to the launches (if launches are appropriately designed) – thus even simplified models without de-embedding or without launch models can be relatively accurate. Though, the technique cannot be used to investigate the limit values or variations of the dielectric constant over the surface of the board (as visible by narrow traces). The technique is suitable for dielectric identification for power-integrity applications, but not for analysis of interconnects.

A good alternative to techniques based on transmission line segments and on the analysis of cavity is technique based on **resonators connected or coupled to a transmission line** [3], [9]. The identification structures can be designed with narrow transmission line segments only to investigate variations of dielectric properties visible by actual interconnects on the board. The corner cases can be investigated in this way. SMA or probe launches can be de-embedded [3], [9] with larger errors than in case of t-line segments because of the resonances are less sensitive to de-embedding errors caused by differences in launches and in the de-embedding test fixtures.

The goal of this project is to define high-confidence design methodology for interconnects on low-cost PCBs fro 6-20 Gb/sec signals. To predict behavior of interconnects, we start with development of a simple and practical procedure to identify broad-band dielectric properties. As in the previous investigations, the methodology is based on comparisons of measured and simulated S-parameters. Though, in addition to transmission line segments, we used in-line resonators similar to technique proposed in [9]. S-parameters are measured with VNA and de-embedded with TRL/LRM procedure.

All test structures were designed with SMA connectors and optimized launches to minimize the de-embedding errors and to increase accuracy of the identification. A new element of the identification is advanced 3D full-wave electromagnetic analysis with causal wide-band Debye dielectric model, broad-band conductor model with roughness, and model for conformal solder mask. After the extraction of dielectric parameters, we used them to investigate typical elements of interconnects such as via-holes, bends, meanders, and so on. All results of electromagnetic analysis are compared with the measured S-parameters de-embedded with TRL/LRM method.

The paper is organized as follows. Overview of the test board is provided in section 2. Different options for dielectric models are analyzed in section 3. Electromagnetic

analysis methodology is described in section 4 and measurements methodology in section 5. After all elements of measurement and simulation are outlined, we introduce the dielectric material identification methodology in section 6. Section 7 contains results of simulation and measurements for some practical interconnect structures. The main results of the project are summarized in section 8.

2. Test board overview

The physical layer reference design board (PLRD-1) is shown in Fig. 2.1 and is designed to provide a set of structures to identify parameters of low-cost FR-4 dielectric and to benchmark electromagnetic analysis software with measurements. There are 30 test structures on the board. Transmission line segments and resonant structures are used to identify dielectric properties. Typical elements of single-ended and differential multi-gigabit data channels and some pedagogical structures are added to benchmark electromagnetic or signal-integrity simulators. All test structures are equipped with well optimized launches from SMA connectors to micro-strip lines. SMA connectors are used instead of probes to make all measurements repeatable and to use the board for methodological and pedagogical purpose.

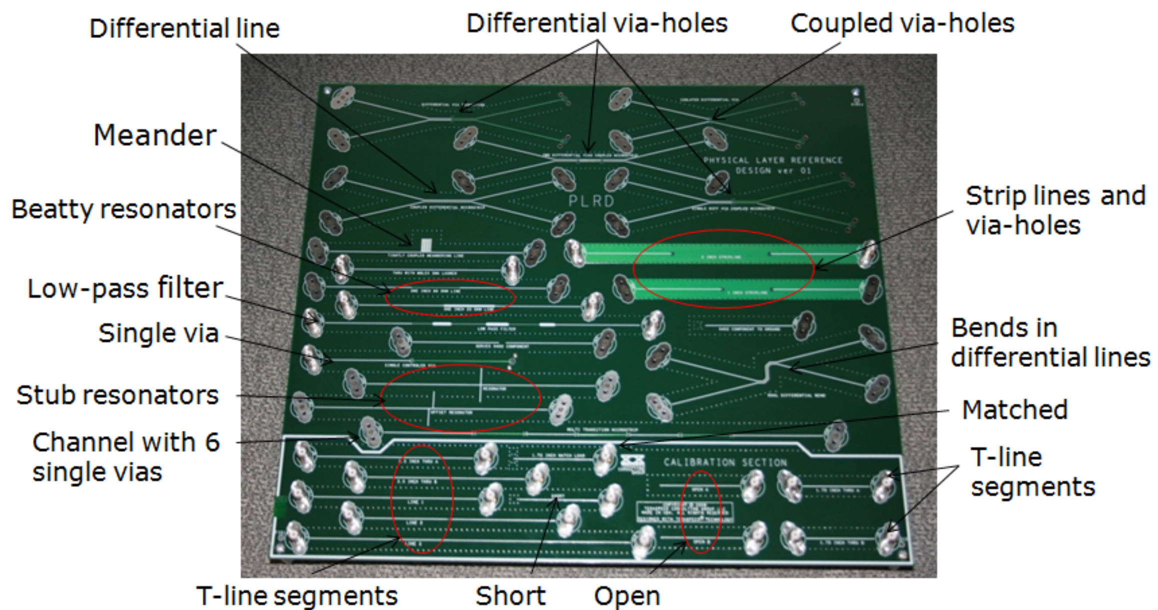

Fig. 2.1. Physical layer reference design board (PLRD-1) with 30 test structures. All structures are equipped with SMA connectors with optimized launch.

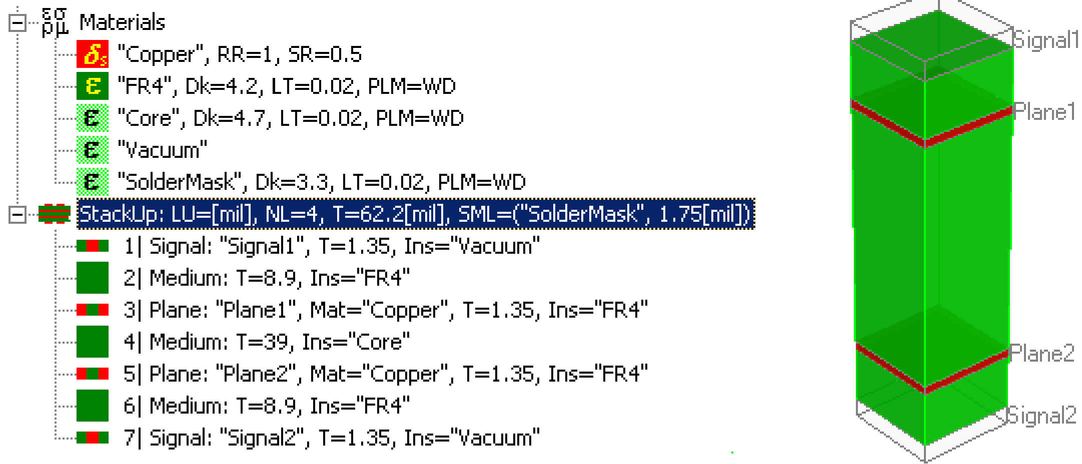

Fig. 2.2. PLRD-1 board materials and stackup.

Board stackup has four layers as shown in Fig. 2.2. Manufacturer of the board provided values 1.724e-8 Ohm*meters for the copper bulk resistivity and 0.5 um for RMS roughness. Roughness factor or RMS ratio of length along the rough surface to the straight line length between two points is guessed to be 2. Conformal solder mask dielectric constant (DK) is 3.3 and loss tangent (LT) is 0.02. FR-4 core dielectric DK=4.7 and LT=0.02. Parameters provided by manufacturer for FR-4 dielectric of the substrate between signal and plane layers are DK=4.2, LT=0.02. **These values will be adjusted on the base of the measurements and simulations.** Measurement frequency for all dielectrics is guessed to be 1 GHz (no data from manufacturer).

3. Selection of dispersive dielectric model

Multiple researches, investigated composite PCB and packaging materials, observed decline of dielectric constant and relatively small growth of the loss tangent over a wide frequency band [7]-[18]. Note that the increase of dielectric constant at higher frequencies observed in [9] and in some other cases can be attributed to non-TEM dispersion in micro-strip lines and not actually to the dielectric properties. The properties of such dielectric can be described with a Debye model with multiple poles [7], [8]. A generalization of such model naturally leads to a simple **wideband Debye** model with infinite number of poles [7], [19] (sometime called **Djordjevic-Sarkar model**). **The model captures the physics of the composite dielectrics, it is causal and requires just two coefficient to describe it and to correlate it with the measurements**. Frequency-dependent complex dielectric constant of the wideband Debye model [7] is defined as:

$$\varepsilon_{wd}(f) = \varepsilon_r(\infty) + \varepsilon_{rd} \cdot F_d(f), \quad F_d(f) = \frac{1}{(m_2 - m_1)\cdot \ln(10)} \cdot \ln\left[\frac{10^{m2} + if}{10^{m1} + if}\right] \qquad (3.1)$$

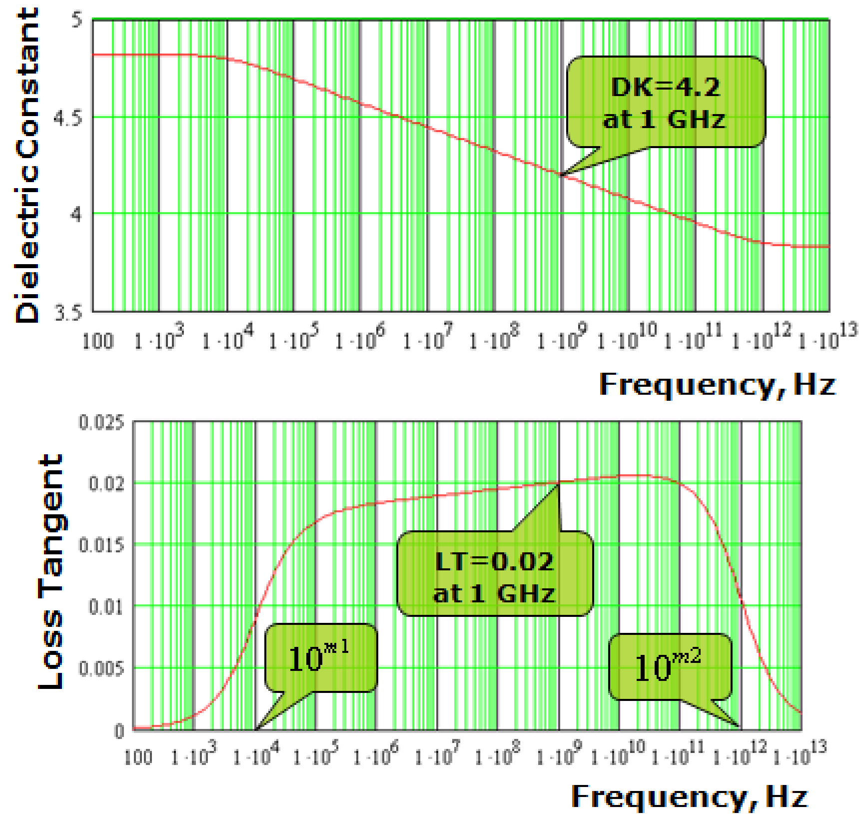

Fig. 3.1. Dielectric constant (top graph) and loss tangent (bottom graph) of wideband Debye model defined with dielectric constant (DK=4.2) and loss tangent (LT=0.02) at 1 GHz (initial data from the PCB manufacturer).

With m1=4 and m2=12 and DK=4.2 and LT=0.02 defined at 1 GHz as for our substrate dielectric, formula (3.1) gives dielectric constant and loss tangent dependencies shown in Fig. 3.1.

Let's explore some other options for the dielectric modeling. Assumption of constant and frequency-independent DK and LT leads to the simplest and widely used dielectric model. This model does not capture the decline of the dielectric constant and results in non-causality of the final model and can be used cautiously only over very narrow frequency band (for microwave applications for instance). The other model used to simulate composite dielectric is Lorentzian model with complex poles [10], [15]. Though practically any causal function can be fitted with the complex poles, there is no evidence that composite dielectrics have complex poles or resonances anywhere close to our frequency band of interest. Thus the Lorenzian model is purely artificial fit and does not capture the physics of the composite PCB dielectric.

Only multi-pole Debye with finite number of poles can be considered as an alternative to the wideband Debye model. Multi-pole Debye model is more flexible, but at least 4-5 poles have to be used for the interconnects analysis. It makes it more difficult to correlate results of transmission line segment or resonator analysis to experimental data – some numerical optimization procedure has to be used to fit computed and measured S-parameters. Thus, **we will use the wideband Debye model**

for the identification of dielectric properties here because of it captures the physics of the composite dielectrics and **very simple to fit to measured data - dielectric constant and loss tangent at one frequency has to be adjusted or swept to fit the model**.

4. Electromagnetic analysis methodology

To support advanced dielectric parameters identification, electromagnetic analysis has to satisfy the following set of requirements (partially formulated in [13]):

- Use **3D full-wave** algorithm for analysis of t-lines and discontinuities
- Have causal dispersive dielectric model – **multi-pole or wideband Debye**
- Have **broadband conductor loss and dispersion models** valid and causal over 4-5 frequency decades (skin, edge, and proximity effects, conductor plating)
- Model conductor **surface roughness**
- Model **high-frequency dispersion** effect
- Extract **de-embedded S-parameters** for discontinuities
- Extract **frequency-dependent RLGC** per unit length parameters for transmission lines

It is practically impossible to satisfy all those conditions if one numerical method is used for the analysis. Thus, we combined the **method of lines and Trefftz finite elements** [22], [23]. Method of lines provides very efficient analysis of multilayered dielectrics and plane interiors and Trefftz finite elements are used to simulate the interior of the strip conductors. Multilayered conductor plating and roughness are taken into account with such approach. Wideband and multi-pole Debye models are used to simulate dispersive properties of the dielectrics. Method of simultaneous diagonalization is used to extract modal and RLGC per unit length parameters from the 3D full-wave analysis of a segment of multi-conductor transmission line and to de-embed S-parameters of discontinuities in these lines [24]. Such analysis accounts for non-TEM properties of the waves in multi-conductor micro-strip lines and provide a frequency-dependent impedance definition that is the closest to the impedance visible from a coaxial cable during the measurements [25]. Transmission line or wave-ports of discontinuities are de-embedded with the method of simultaneous diagonalization to eliminate numerical test fixture and to increase accuracy of the de-compositional analysis.

Conductor surface roughness is modeled with the local adjustment of conductor surface impedance on the base of measured root-mean-square distance from peak to valley (roughness or SR) and ratio of distance along the rough surface to straight line (roughness factor or RF) as illustrated in Fig. 4.1.

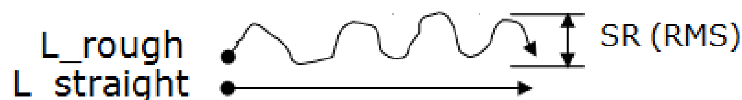

Fig. 4.1. Measurement of conductor surface roughness and roughness factor.

Trefftz finite elements and the local impedance adjustment technique make it possible to distinguish the surface roughness on the opposite surfaces of the strip that is often the

case in PCB manufacturing industry and creates very specific attenuation pattern. **This advanced conductor roughness model increases accuracy of the analysis and improves quality of the dielectric parameters identification**. As an example of roughness effect, attenuation in a strip-line is plotted as function of surface roughness in Fig. 4.2 for four frequencies and roughness factor 2. With this roughness factor, the attenuation may increase 2 times and cannot be neglected in the dielectric properties identification at high frequencies.

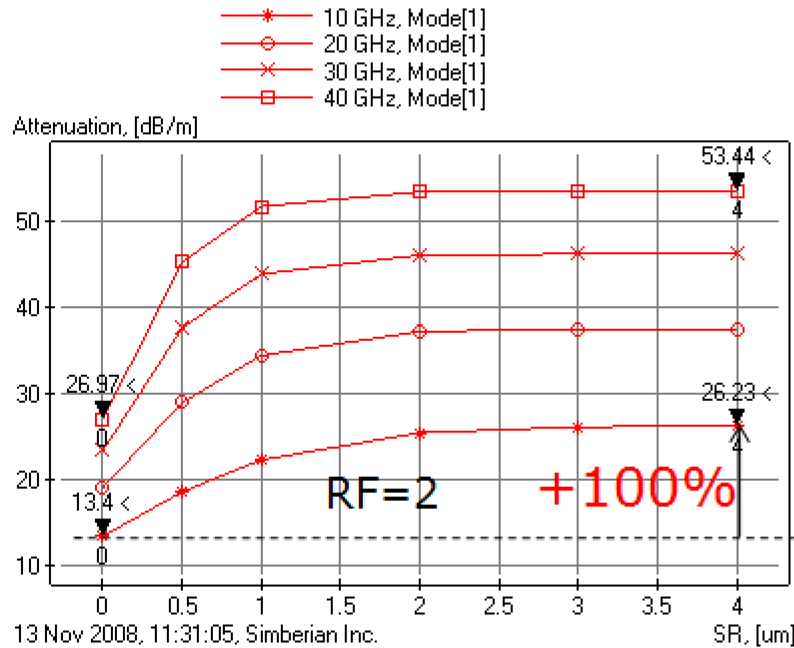

Fig. 4.2. Attenuation in strip-line versus surface roughness in micrometers for four frequencies. Roughness factor is 2.

Full-wave 3D analysis of complicated interconnect structures from one connector to another as a whole is possible, but not very practical solutions due to large number of fine details to resolve and dispersive conductor and dielectric properties. An alternative to analysis as a whole is the **full-wave multi-modal de-compositional analysis of the interconnects**, originally developed for wave-guiding problems in [20], [21]. A channel is de-composed into elements such as transmission line segments and discontinuities or transitions.

Then **full-wave models have been built with different level of approximation for transmission lines and discontinuities and re-composed into a full-wave model of the complete channel**. Transmission lines constitute major part of any channel, thus the accurate analysis and parameters extraction that accounts for all kinds of losses and dispersion is important for the modeling of t-line segments. Following this procedure, we extract models for t-lines and discontinuities first, and then use them as the building blocks to simulate different structures on the test board using linear frequency-domain analysis to connect corresponding multiports. To perform all this tasks we used Simbeor 2008 software [27] that satisfies all requirements for the material parameters extraction listed in the beginning of this section.

Because we used the appropriate dielectric model we are able to extract frequency-dependent properties of dielectrics and to provide very close correspondence between measurement and resulting simulation.

5. Measurement methodology

A simple SOLT calibration at the coaxial ports of the netweork analyzer removes the effects of the network analyzer, cables, and any associated adapters before the fixture. This does not account for the fixture itself consisting of the SMA launch to transmission line and transition into the device. During this study we compared several approaches to either de-embed or calibrate the fixtures error, which included:

- **Calibration –**
    a. **SOLT** (Short-Open-Load-Thru) and TRL(Thru-Reflect-Line) . SOLT measures 4 on board standards that can be used to provide DUT only s-parameters where a 12-term SOLT error model is used. On board calibration kits are very difficult to characterize accurately.
    b. **TRL** uses Thru, a Reflect, and Lines to perform calibration. Standards are easy to calibrate, such that the impedance and delay of each Line must be known. Several Lines cover a broad frequency range defined by a span of frequencies.
- **Error correction -** Shifts the magnitude/phase to the device. In fixture THRU lines provide ability to use VNA internal memory to subtract the fixtures' effect from the measurement. Return loss performance and 1% modeled-measurement correspondence is not possible using low cost FR-4 to 20GHz using this method.
- **De-embedding** - Mathematical process such as T-matrix or ABCD matrix approach where raw SOLT calibrated S-parameters are post-processed. Requires a given or known response for the fixture error and associated EDA software such as ADS2008.

The Agilent N5230A 4-port network analyzer was used to measure S-parameters of one-two and four-port structures on the test boards. Considering the performance required in making very accurate measurements to 20GHz two methods immediately emerged as top choices for removing fixturing effects of the final device S-parameters: **T-matrix de-embedding, and TRL calibration.** ADS2008 software [27] was used to import S2P TRL calibrated data from VNA and compare this to T-matrix de-embedded data. S2P blocks were imported using Data blocks in ADS2008.

For both TRL and T-matrix fixture removal effects, the THRU measurement provided a comparison to validate the repeatability of the standards. The simple THRU S-parameter measurement was measured to compare the approaches where the ultimate goal was zero insertion loss, zero delay, zero phase, and low return loss of the THRU calibration measurement after either de-embedding or calibration. Comparison of the two de-embedding techniques is shown in Fig. 5.1. TRL provided better insertion loss, delay, but not better return loss for the THRU calibration structure measurement. It can be explained by the assumption of negligible reflection during the TRL calibration.

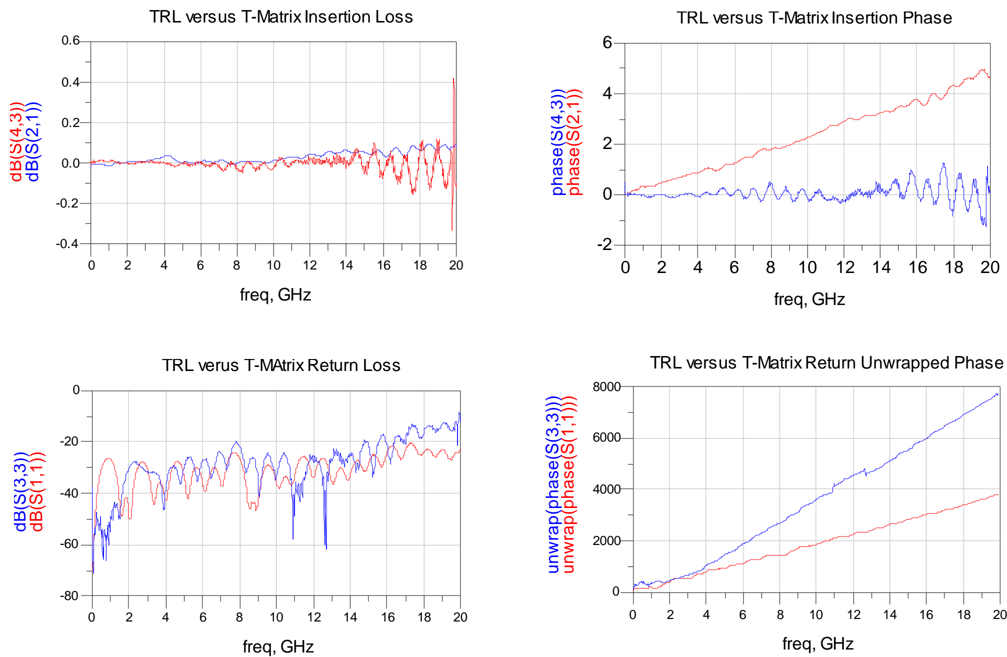

Figure 5.1 **THRU measurements.** Comparison of T-matrix de-embedding (red line) with TRL/LRM calibration (blue line).

Comparison of the T-matrix de-embedding method and TRL/LRM suggests that TRL/LRM is the most accurate technique for generating correspondence S-parameter data for 3D electromagnetic modeling

Establishing the Calibration TRL/LRM kit is fairly straightforward in that you initially define the highest frequency of interest. Typically, even though 20GHz bandwidth for many applications is not required, this is the maximum frequency for the N5230A VNA that we used, so we arbitrarily selected a frequency greater than that. The lowest frequency band is defined by the longest line which typically starts at 100-200MHZ. A low band 50ohm load was used for LOAD and was verified to have good return loss, S11 past 200MHz. Note that the MATCH (for LRM – LINE, REFLECT, MATCH) for TRL/LRM provides calibration down to 0Hz without utilizing an inconvenient LINE length of infinity (a MATCHED line electrically mimics an infinite length line, neglecting losses of course). This data is then entered into the spreadsheet developed by Molex Corp. as shown in Fig. 5.2 (permission granted by Dave Dunham).

Inputs:	Effective Dk	Reference Length(mm)	Reference Length(in)	Frequency Ratio	Low Phase	High Phase
	3.2	44.45	1.75	5	30°	150°

Outputs	Start Frequency (Ghz)	Stop Frequency (Ghz)	Time Delay (ps)	Line Length (mm)	Line Length (in)
Short/Open			0	44.45	1.75
Load	0	183.31	0	44.45	1.75
Line 3	183.31	916.55	454.61	165.0873	6.4995
Line 2	917.92	4589.6	90.79	104.1146	4.099
Line 1	4585.76	22928.8	18.17	91.94546	3.6199
Thru			0	88.9	3.5

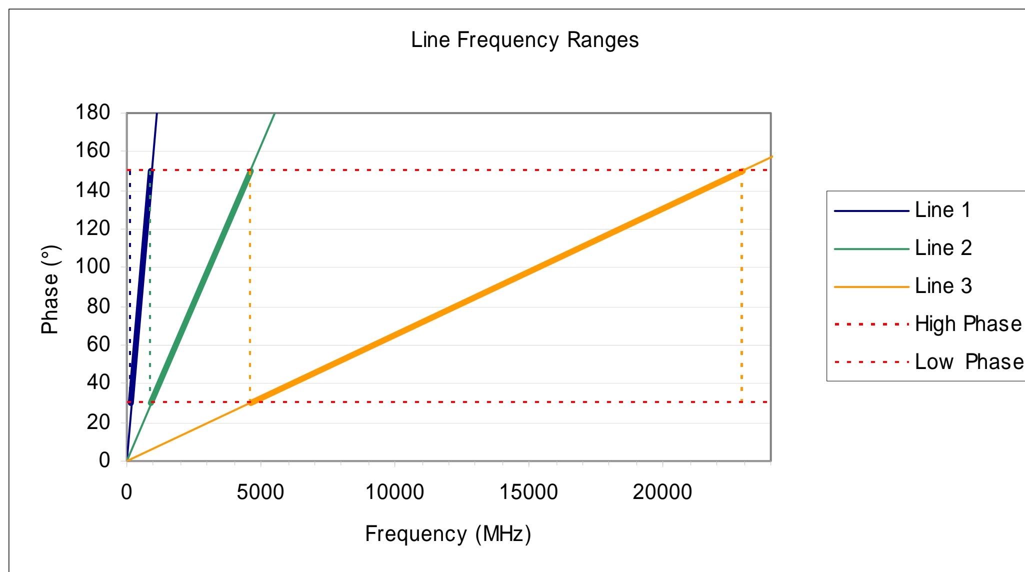

Figure 5.2 Molex spreadsheet eases TRL/LRM LINE length calculations. PLRD-01 incorporates a 4th LINE of infinite equivalent length, a MATCH which is 50ohm terminated with an Agilent cal-kit Low-Band 50ohm load with a ½ length THRU.

The quality of the outlined TRL de-embedding procedure can be illustrated by S-parameters of the THRU structures. Ideal de-embedding of zero-length transmission lines produces S-parameters with transmission coefficient with unit magnitude (0 dB), zero phase and zero group delay. There must be zero reflection from THRU. Deviations from those values characterize the de-embedding errors. Magnitude of the transmission coefficient deviates from 0 dB only by 0.02 dB and phase deviates from 0 by 0.24 degrees and the reflection is well below -50 dB for all frequencies. Group delay error is bounded by 1.2 ps as shown in Fig. 5.3. Differences between magnitudes and phases of the two transmission coefficients S[1,2] and S[2,1] is non-reciprocity of the measurement procedure. The non-reciprocity is very small – maximal difference in magnitudes was 0.004 dB and in phases is 0.07 degrees. There is also very small violation of the expected symmetry properties of THRU S-parameters (equality of the reflection coefficients S[1,1] and S[2,2]).

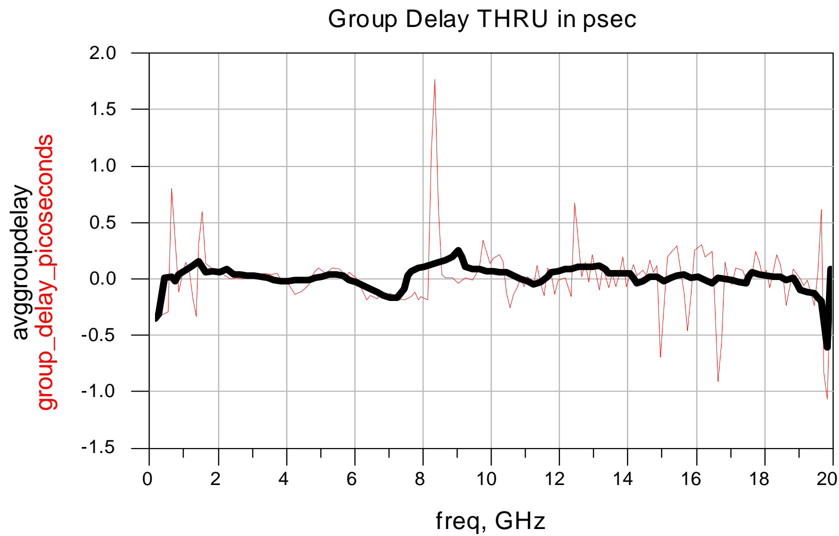

Figure 5.3 TRL/LRM THRU group delay boxcar averaged

Small errors illustrate high quality of the developed de-embedding methodology. The measured data can be safely used to extract dielectric parameters with high accuracy and to use measured S-parameters to benchmark the electromagnetic analysis.

TRL/LRM S-parameter calibrated data was post-processed exploiting symmetries, reciprocity and passivity of the structures:

- Structure has 1st order geometric **symmetry** if (left half)=(right half), or reflection coefficients are equal: **S11=S22**
- Structure is **reciprocal** if no anisotropic materials used or **S21=S12**
- Structure is **passive** if no energy generated of *eigenvals*(**S**)<=**1.0**

In each case all those quality was also insured by careful calibration methods and enforced in post-processing if necessary.

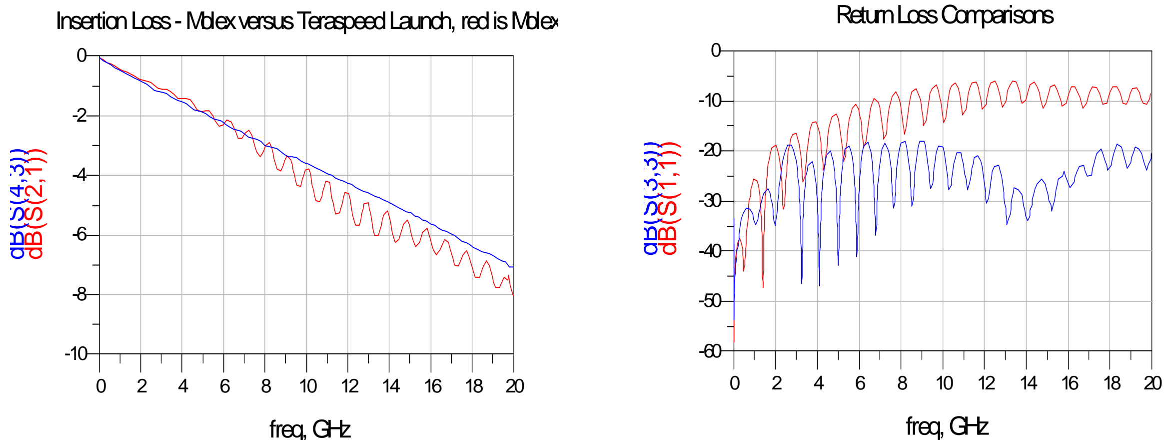

Figure 5.4 TRL/LRM calibration is very sensitive to launch resonance and poor return

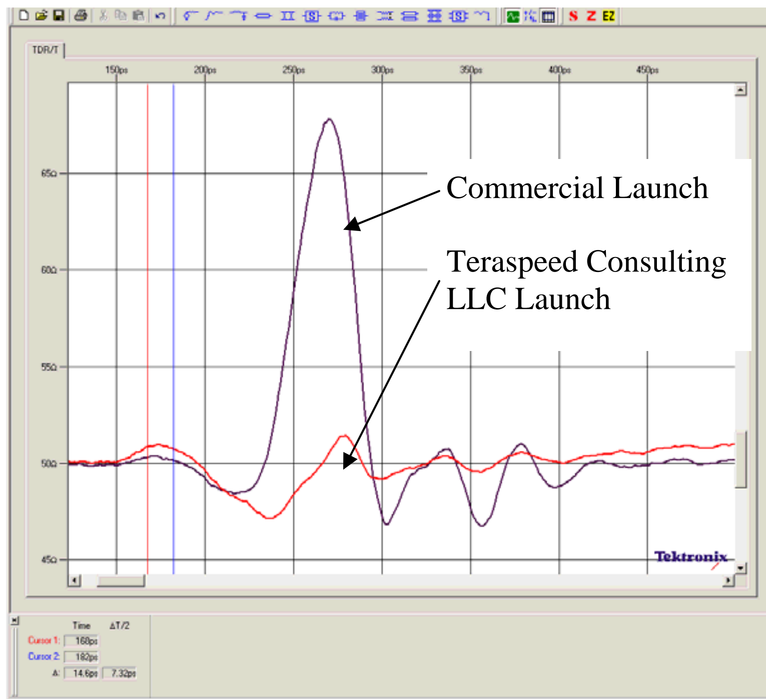

Figure 5.5. TDR comparison of pristine launch used and commercially suggested launch, both using Molex surface mount SMA. TRL cannot calibrate 150psec of resonance with large impedance variation for launch.

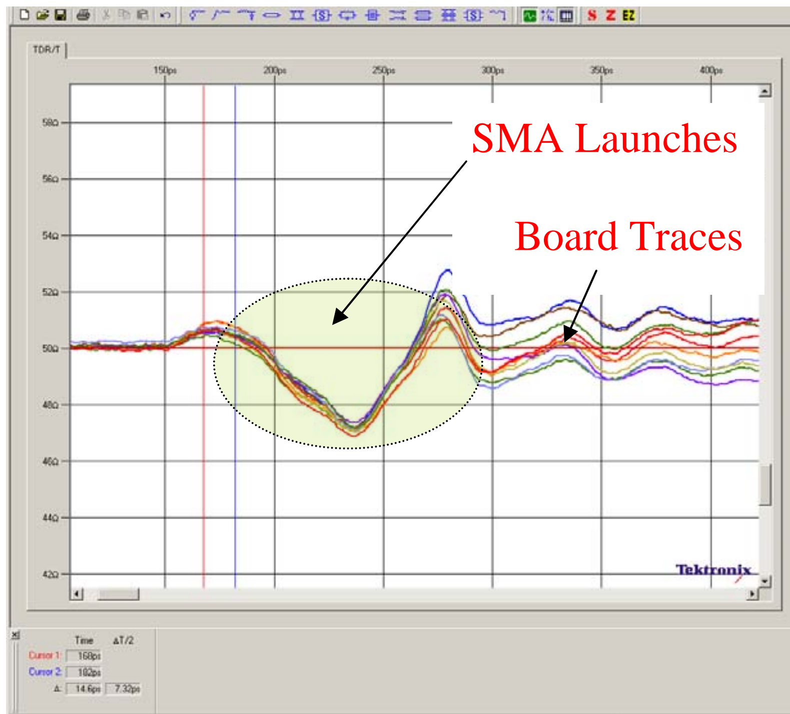

Figure 5.6. A TDR was performed on every SMA launch and overlaid. Consistent SMA launch repeatability was a critical step for insuring a good TRL calibration set and subsequent calibrated measurements for all devices.

One of the most important elements of the measurement setup is the SMA launch. For successful de-embedding the launches must have as small reflection as possible and the differences between launches for different structures on the board must be minimized. The launch suggested by the connector manufactured was optimized to minimize the reflection. Fig. 5.4 and 5.5 compare the original and optimized launches. The optimized launch has reflection below -19 dB over all frequency band and almost no oscillations in the transmission coefficient. Fig. 5.6 compares the optimized launches for multiple structures on the board and shows good correlation necessary for successful de-embedding.

6. Identification of dielectric parameters

To identify dielectric properties we first **measure and de-embed S-parameters** of two classes of structures:

- **Line** segments or low reflective structures (very low S[1,1])
- **Resonant structures** or high reflective structures with clear resonances in S[1,1]

Next we create a full-wave model of the structures with wideband Debye dielectric model and fit the model at one frequency (1 GHz for instance) as follows:

- **Sweep DK @ 1 GHz and find value with the best correspondence of resonances and transmission coefficient phase and group delay**
- **Sweep LT @ 1 GHz** and find value with the best correspondence in **transmission coefficient magnitude**

We start with transmission line segments or low-reflective structures. Micro-strip line in layer Signal1 of stackup shown in Fig. 2.2 has strip width 17 mil (about 50 Ohm by design). Line segment is 3 inch long after the test fixture is de-embedded. Dielectric constant in the full-wave model is adjusted to 4.15 at 1 GHz to match the measured transmission coefficient phase and loss tangent is adjusted to 0.018 at 1 GHz to match the measured transmission coefficient magnitude. The final results are shown in Fig. 6.1. Considering the reflection from the transmission line segment, the transmission line has impedance close to 50 Ohm that makes reflection coefficient very small and sensitive to all even small de-embedding errors. As the result, non-symmetry in S-parameter coefficients S11 and S22 was observed and multiple minima in addition to the minima expected at frequencies when line segment length is proportional to quarter of wavelength. The reflection coefficient magnitude is shown in Fig. 6.2 after the enforcement of symmetry and filtering. Overall the average magnitude of the measured reflection corresponds to the simulated that means that the line impedances of simulated and measured lines are very close.

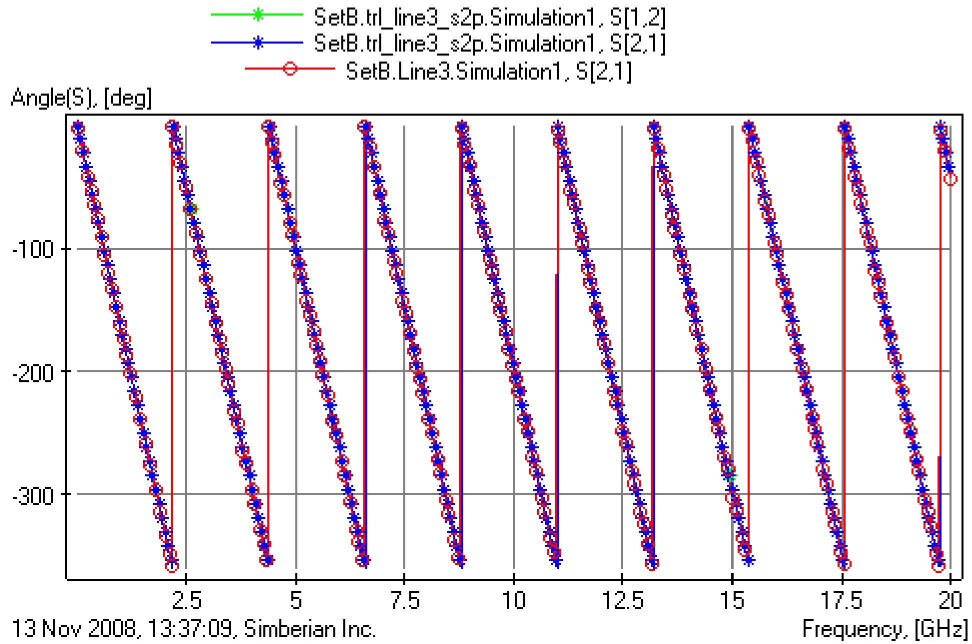

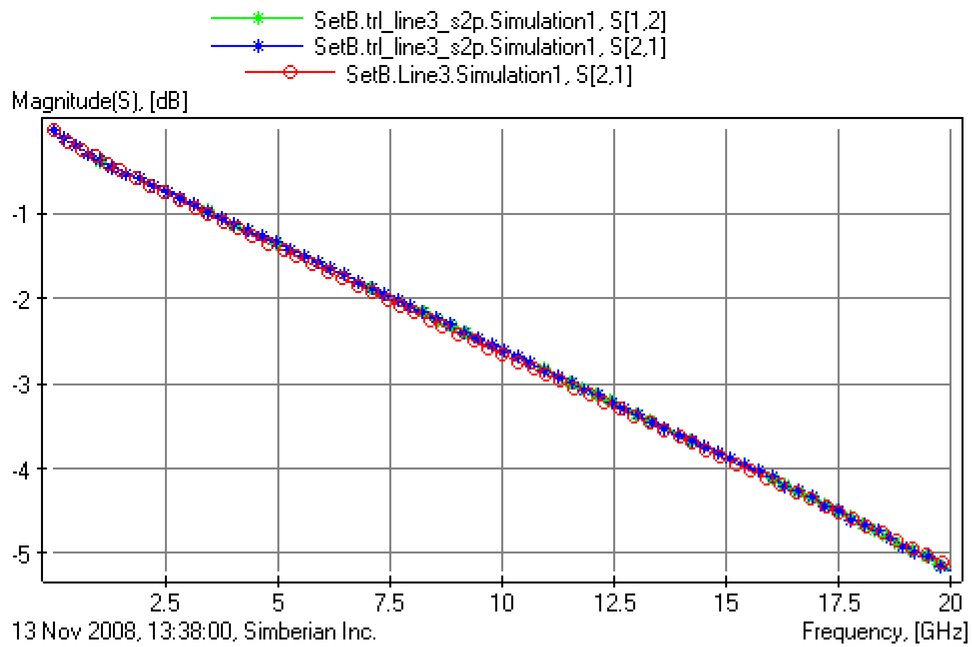

Fig. 6.1. **17 mil wide and 3-inch long segment of micro-strip line:** correspondence of measured (stars) and simulated (circles) phases of the transmission coefficients (top graph) and magnitudes of the transmission coefficients (bottom graph) after adjustment of DK to 4.15 and LT to 0.018 at 1 GHz.

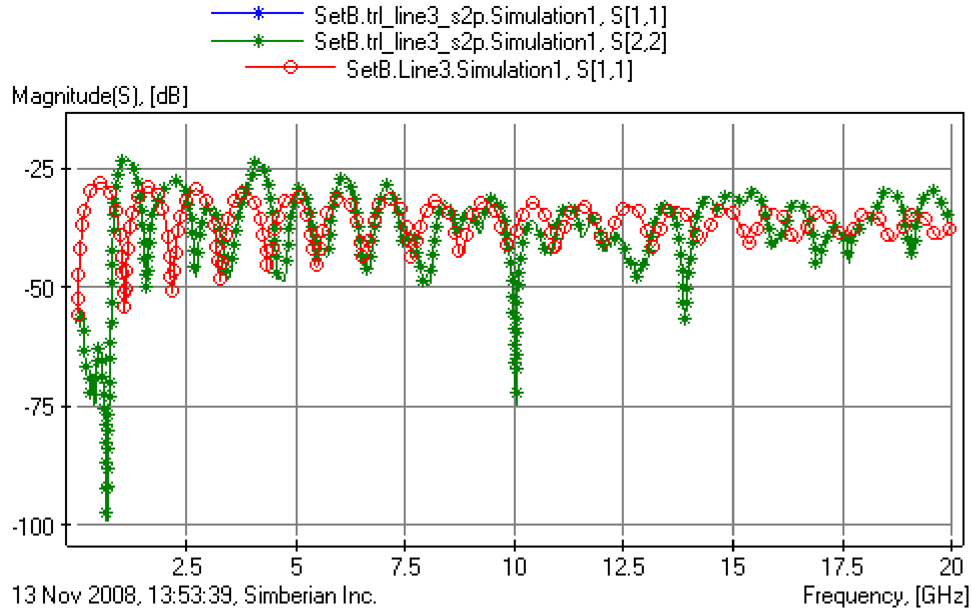

Fig. 6.2. **17 mil wide and 3-inch long segment of micro-strip line:** correspondence of measured (stars) and simulated (circles) magnitudes of the reflection coefficients after enforcement of symmetry and filtering (DK is 4.15 and LT is 0.018 at 1 GHz).

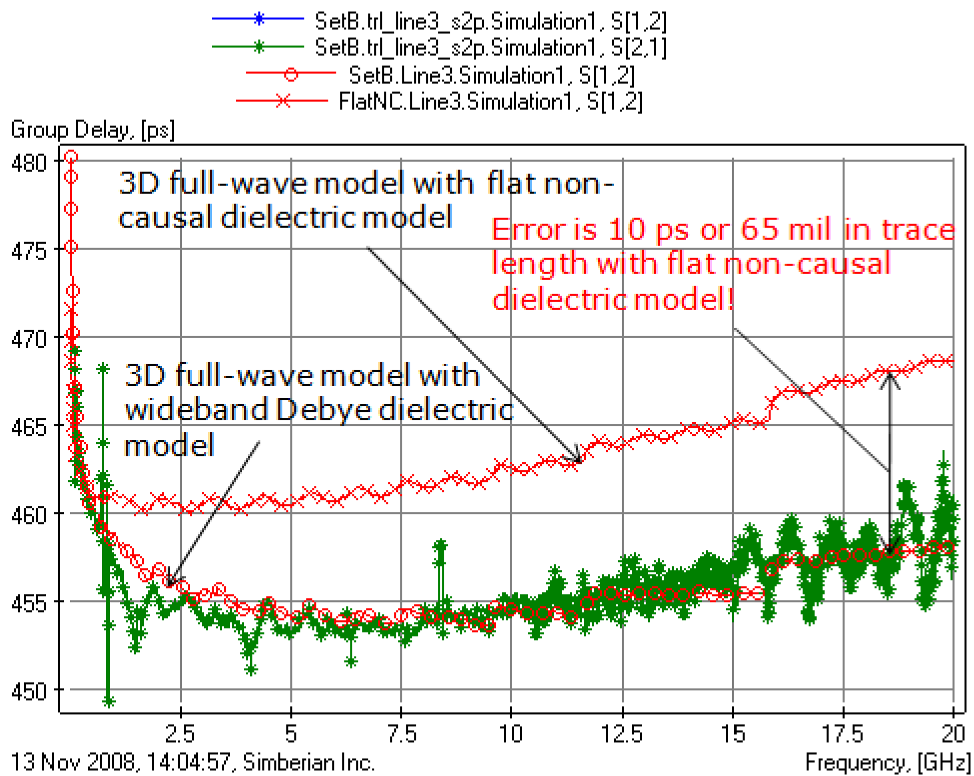

Fig. 6.3. **17 mil wide and 3-inch long segment of micro-strip line:** comparison of group delays of measured (stars), simulated with wideband Debye model (circles), and simulated with flat non-causal dielectric model (x-s) after enforcement of reciprocity and filtering measured data (DK=4.15 and LT=0.018 at 1 GHz for both models)

To verify that the selected Debye dielectric model works, we simulated the same micro-strip line segment with the flat non-causal dielectric model (DK and LT do not change with the frequency). The results of the comparison are shown in Fig. 6.3. Group delay is identical in two models only at 1 GHz. With wideband Debye model we can see the decline of group delay up to 5-6 GHz due to the decrease of the dielectric constant in wideband model as illustrated in Fig. 3.1. Group delay grows both in model and in experiment starting from 5-6 GHz due to **high-frequency dispersion in micro-strip line**. The difference reaches 10 ps (65 mil in trace length) at 15-20 GHz range. Phase delay difference between causal and non-causal model reaches 65 degrees at 20 GHz. Note that we compare two 3D full-wave models here that differ only in dielectric model.

The difference may be much larger if a static field solver is used to simulate the line, because of the inhomogeneous dielectric effect and dispersion observed above 5 GHz can be captured only with the full-wave analysis of the segment. There is good correspondence of the measured phase and group delay with 3D full-wave analysis with wideband Debye model. Note that oscillation in the measured group delay observed in Fig. 6.3 are due to in-homogeneities of dielectric along the line (glass fibers and resin effect) that can be seen on TDR response and proved with simulation of a model with variation of dielectric constant along the line. There were 4 segments of micro-strip lines investigated in the same way and dielectric parameters identified for each segment. **We observed variation of dielectric constant from 3.9 to 4.25 and loss tangent from 0.018 to 0.02 both at 1 GHz.**

The second set of the identification experiments was with different resonant structures with high reflection. Two Beatty standards and two stub resonators have been investigated. The first resonator is so-called Beatty standard with 1-inch segment of 25 Ohm micro-strip line connected in series into 50-Ohm micro-strip line as shown in Fig. 6.4.

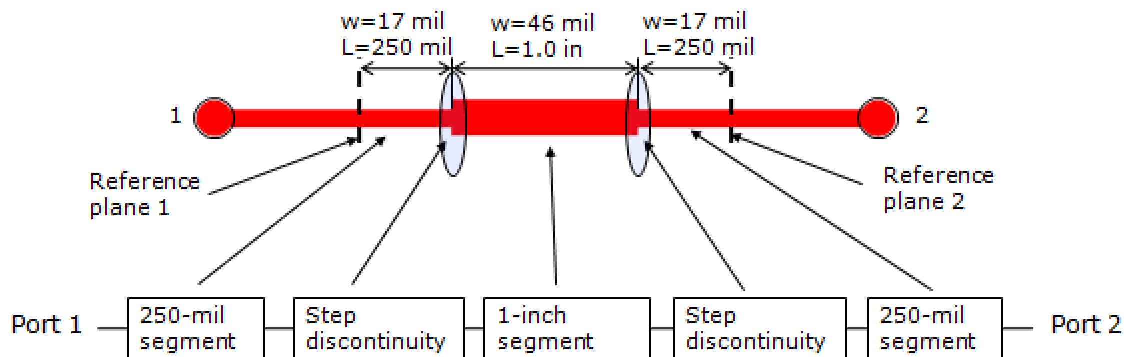

Fig. 6.4. Geometry of Beatty standard with 25-Ohm section of micro-strip line and schematic for de-compositional electromagnetic analysis.

The central segment is bounded by two step discontinuities and transitions to higher impedances – that produces resonances in the reflection coefficients at frequencies when the wide segment length is proportional to half of the wavelength in the segment. After preliminary analysis of the 46 mil wide micro-strip in Signal1 layer of the stackup shown in Fig. 2.2 we can predict the lowest resonance at about 3.23 GHz (half wavelength) and

the last resonance in our frequency band at about 19.44 GHz (three wavelengths). The positions of the resonances are mostly affected by changes in dielectric constant with frequency (smaller dielectric constant increases the resonance frequency) and by the effects of the step discontinuities (step makes the resonator appear a little longer that decreases the resonance frequency).

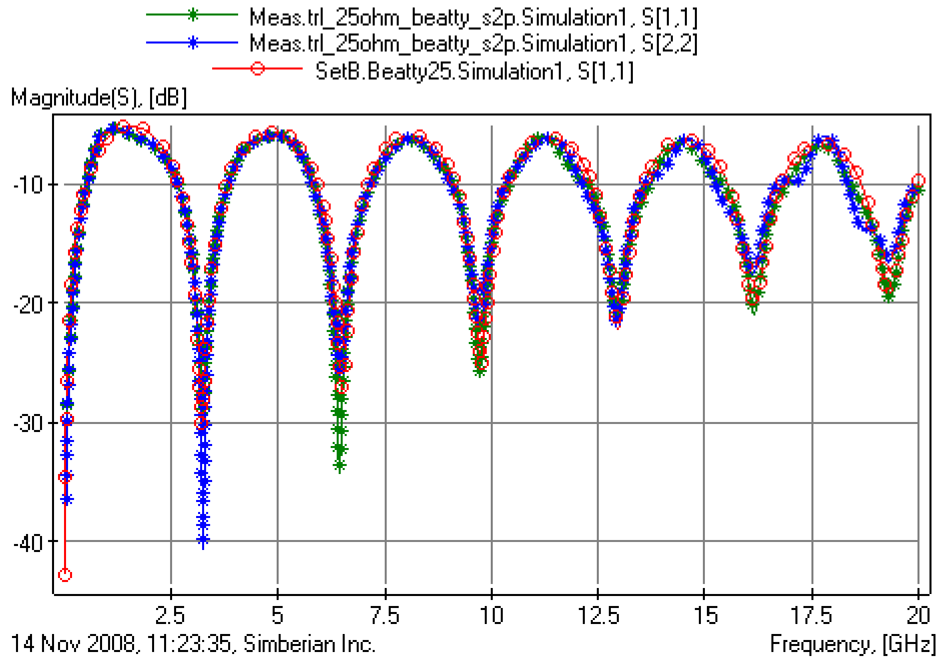

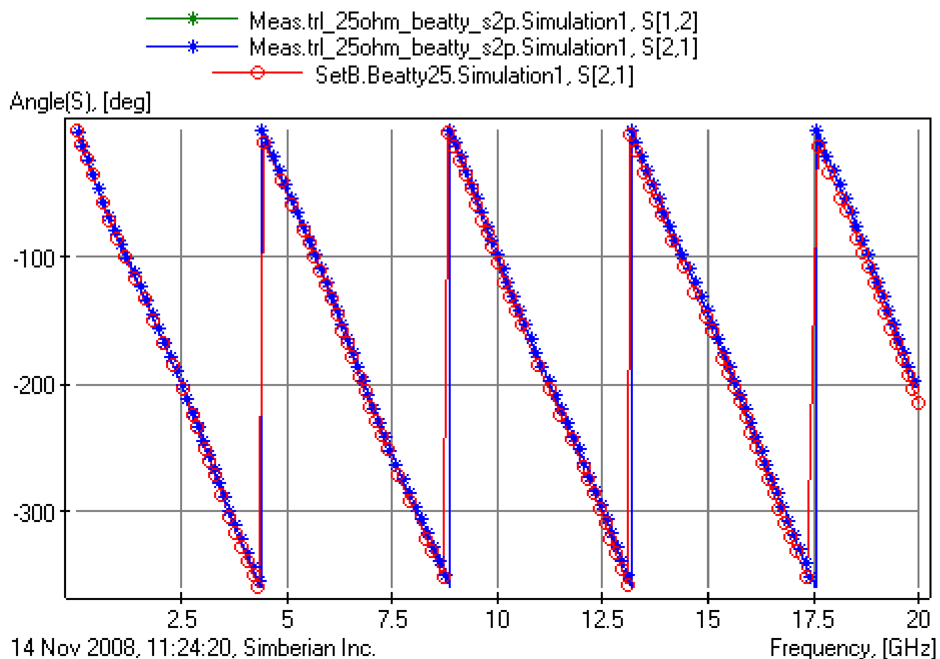

Fig. 6.5. **25 Ohm Beatty standard:** correspondence of measured (stars) and simulated (circles) magnitudes of reflection coefficients (top graph) and phases of the transmission coefficients (bottom graph) after adjustment of DK to 3.9 at 1 GHz (LT=0.018).

To account for both effects we first extract broadband RLGC(f) per unit length parameters of 17-mil and 46-mil micro-strip lines. Then we extract S-parameters of the step discontinuities to model the junction between two lines. Both extractions are done with 3D full-wave analysis and with wideband dielectric model with initial guess of DK=4.2 and LT=0.02 at 1 GHz. Finally we recompose the models for lines segments and for the step discontinuities as shown in Fig. 6.4 and compute S-parameters of the structure to compare them with the experimental data. Note that simulation of a complete structure with all electromagnetic extraction was done within few seconds. We compare the reflection coefficient first and adjust DK to 3.9 @ 1 GHz to match the resonant frequencies in the reflection coefficient and phase of the transmission coefficient as shown in Fig. 6.5. Then loss tangent has been adjusted to 0.018 at 1 GHz to match the measured magnitude of the transmission coefficient as shown in Fig. 6.6.

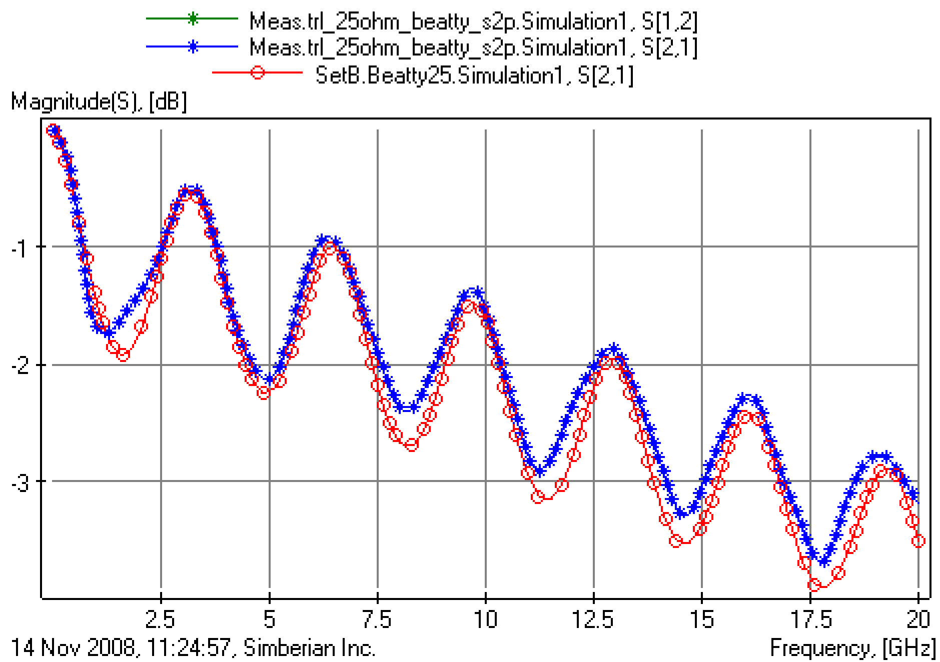

Fig. 6.6. **25 Ohm Beatty standard:** correspondence of measured (stars) and simulated (circles) magnitudes of the transmission coefficients after adjustment of LT to 0.018 at 1 GHz (DK=3.9).

The reflection coefficients S[1,1] and S[2,2] in the top graph of Fig. 6.5 are slightly not equal that means that the mirror symmetry of the structure is violated (the reflection symmetry plane divides the structure vertically in two identical halves). It may happen due to un-symmetry in the de-embedded fixtures or due to the inhomogeneous dielectric along the transmission lines. Finally we check the phase of the reflection coefficient and group delay and conclude that the extracted dielectric model provides good agreement to the measured results. The final dependencies of dielectric constant and loss tangent versus frequency for the extracted dielectric model are shown in Fig. 6.7. **We can observe more that 10% variation in the dielectric constant over the frequency band of interest – it cannot be neglected in analysis of interconnect links.**

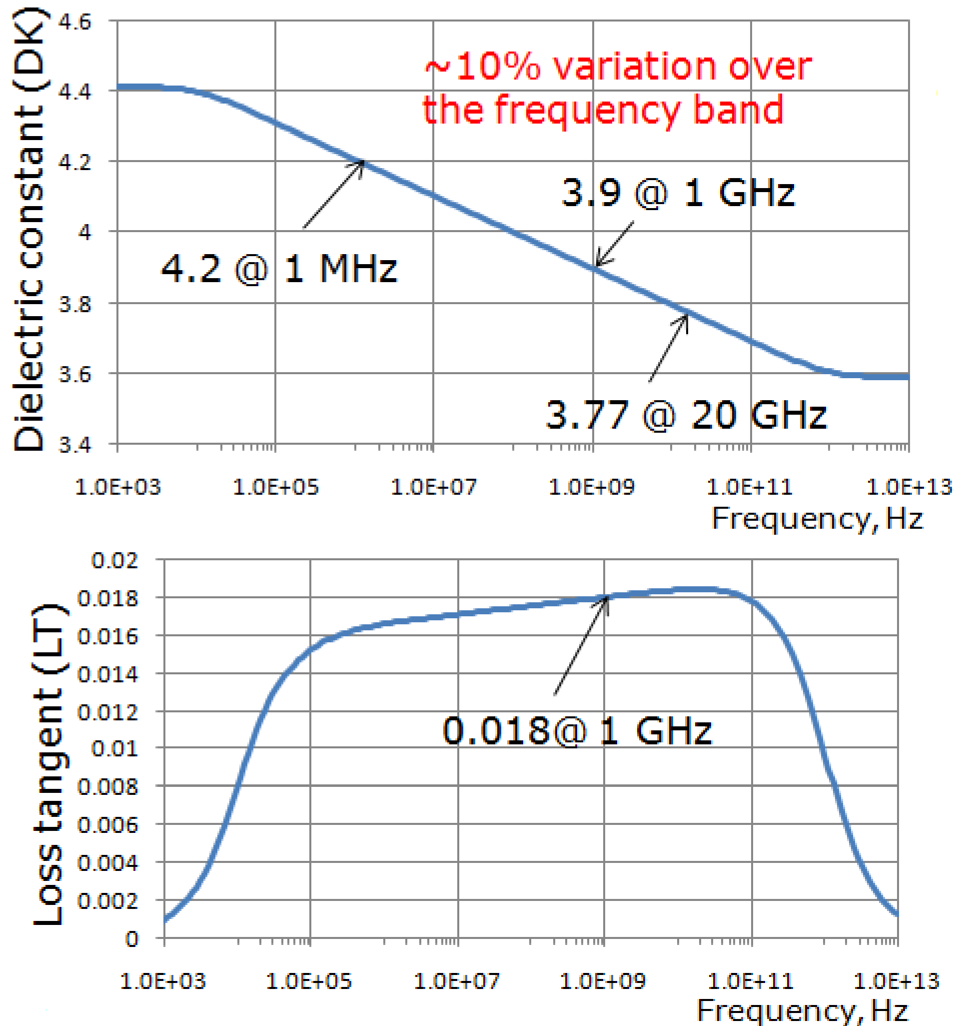

Fig. 6.7. Final broadband dielectric model extracted with 25-Ohm Beatty standard.

To confirm the choice of the wideband Debye model, we constructed same 3D full-wave model of the 25-Ohm Beatty standard with the flat non-causal dielectric model with the same values of dielectric constant DK=3.9 and LT=0.018 (frequency-independent). **The result is the shift of the last resonant frequency by 350 MHz down and 40-degree difference in transmission phase at 20 GHz – this is with 1 inch segment!** With 3-inch resonator we expect about 1 GHz shift in the highest resonance frequency that cannot be neglected. This effect can be obfuscated in the non-causal model by selecting a high dielectric constant for instance and spreading the differences in resonances over the frequency band. It leads either to increase of the first resonance frequency or decrease of the last observed resonance frequency. Holtzman [9] divided frequency band from 2 to 15 GHz into 3 sub-band to have correspondence of simulations obtained with flat non-causal dielectric model with the measurements. Note that the decrease of dielectric constant in micro-strip line is partially compensated by the high-frequency dispersion (concentration of the field in dielectric below micro-strip). **It means that the resonance shift will be considerably larger for a strip line structures because of absence of high-frequency dispersion compensation.**

How relevant is it to the analysis of a real data channel? Via-holes or other transitions in multi-gigabit data channels play the role of discontinuities creating resonances in the channel. **Accurate prediction of these resonances is very critical, because of it is practically impossible to fix the signal degradation caused by such resonances using any pre-emphasis or equalization technique if resonance coincide with an important harmonic of the signal.**

There were 4 resonant structures investigated in the same way as the Beatty 25-Ohm standard and dielectric parameters identified. **With the resonant structures we observed variation of dielectric constant from 3.9 to 4.0 and loss tangent from 0.018 to 0.02 both at 1 GHz.** The smaller variation of the dielectric constant obtained with this methodology supports conclusion on lower sensitivity of this type of extraction to imperfections of the test fixture to the de-embedding procedure [9]. Note that such clean extraction procedure would be impossible without high-quality de-embedding of measured S-parameters because of resonances caused by transitions from coaxial to micro-strip lines. Combination of multiple resonances caused by four discontinuities (two launches and two steps) makes reflection coefficient not acceptable for precise extraction of dielectric properties by matching the resonant frequencies.

7. Comparisons of measurements and simulations

After we identified the dielectric loss and dispersion model and established the limits for dielectric constant and loss tangent variations, we are ready to perform analysis of different structures on the board and compare the simulation with the measurement results.

The first structure is meandering line shown in Fig. 7.1. Such structure can be used as a delay line for instance. The structure can be analyzed either a whole or by the de-composition into a segment of 8-conductor line and two transitional structures above and below the dash lines in Fig. 7.1. The de-compositional modes is as accurate as the direct analysis, but about 100 times faster. 3D full wave model of the 8-conductor line contains delayed coupling along the X-axis, unlike static models typically used in SI software. In addition, the transitional structures account for the effects of bends and coupling between the bends. Those effects are typically neglected in simplified static models, but produce a stop-band filtering effect as shown on the top graph in Fig. 7.2 that can degrade even 5 Gb/s signal in such structure. Though there are some discrepancies in the reflection coefficients at lower frequencies, correspondence of the measured and simulated results is acceptable for practical purpose. Comparison of group and phase delay through the meandering line is provided on the bottom graph in Fig. 7.2. Considerable deviations from behavior of a line segment with the same length as the meander can be observed at frequencies starting from 5 GHz.

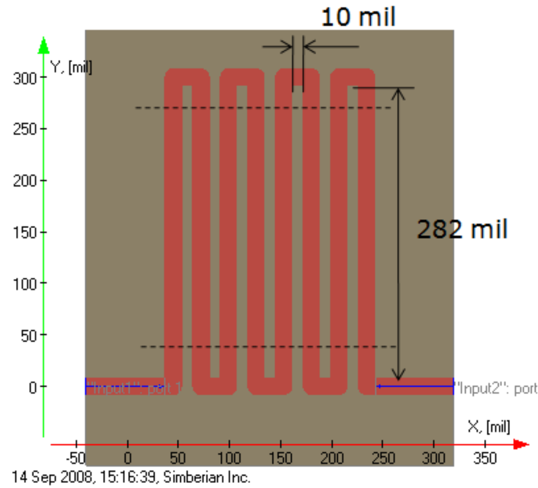

Fig. 7.1. Geometry of meandering 17 mil micro-strip line. 390 mil segments of micro-strip line added on both sides of meander for consistency with the measured structure.

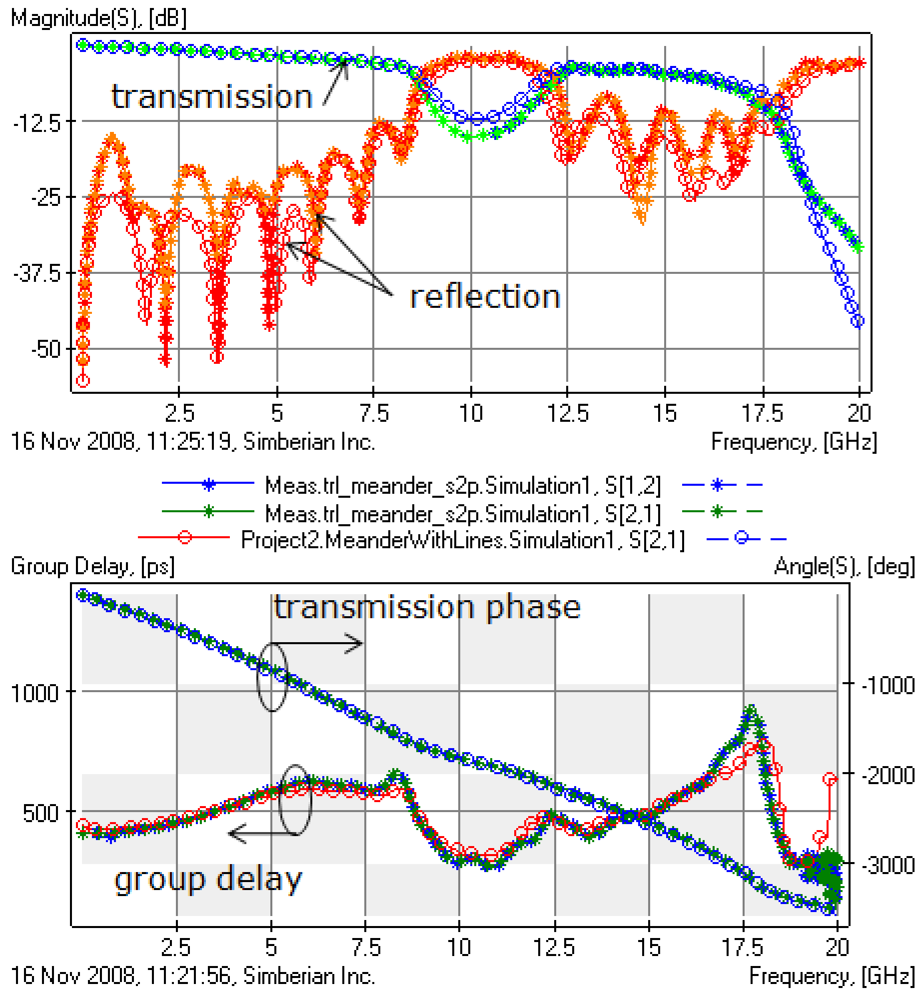

Fig. 7.2. **Meandering 17 mil micro-strip line:** comparison of measured (stars) and simulated (circles) magnitudes of the transmission and reflection coefficients (top graph) and group and phase delays (bottom graph) with DK=4.0, LT=0.02 @ 1

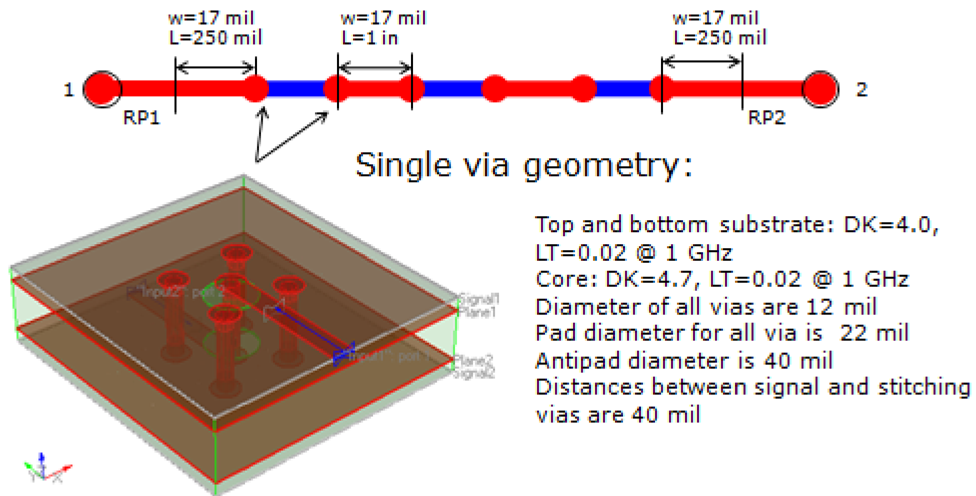

GHz.

Fig. 7.3. Geometry of a micro-strip channel with 6 via-hole transitions through the board. Reference planes are designated as RP1 for port 1 and RP2 for port 2.

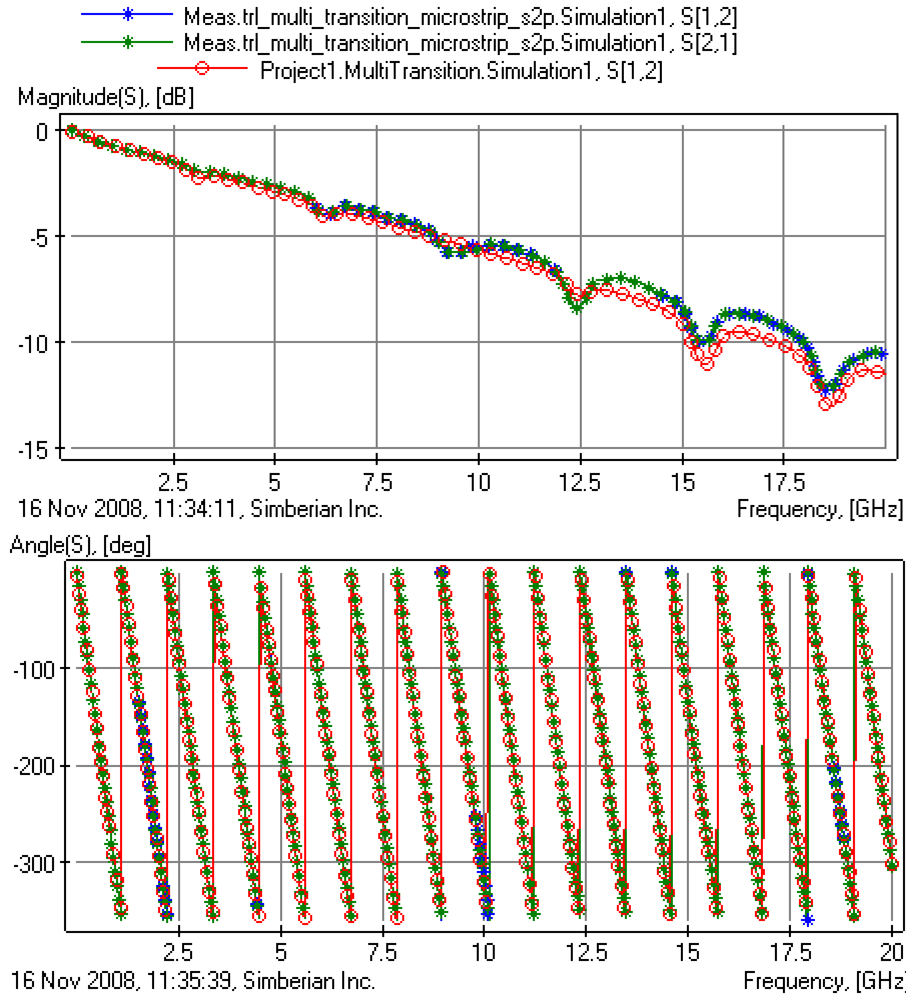

Fig. 7.4. **Micro-strip channel with 6 via-hole transitions through the board:** comparison of measured (stars) and simulated (circles) magnitudes (top graph) and phases (bottom graph) of the transmission coefficients.

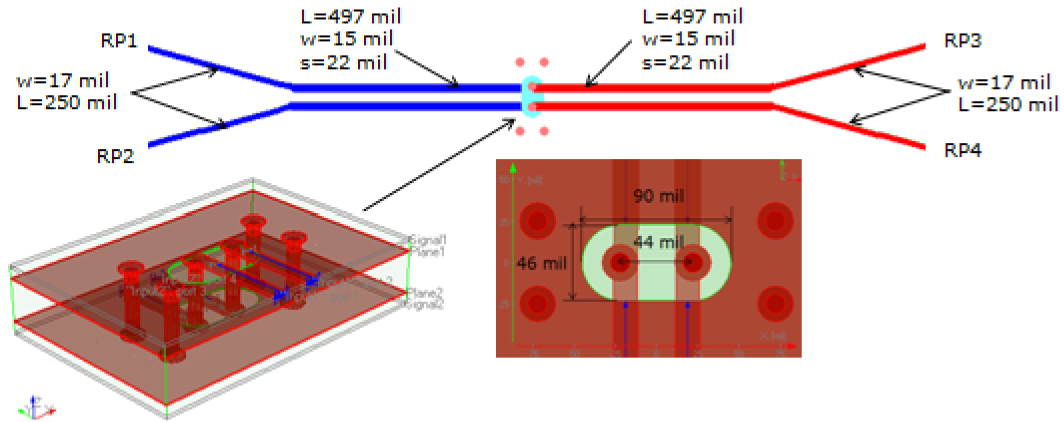

Fig. 7.5. Differential micro-strip lines with differential via-holes. Top and bottom substrate DK=4.25, LT=0.02 @ 1 GHz; core DK=4.7, LT=0.02 @ 1 GHz; 15 mil strips separated by 22 mil; diameter of vias is 12 mil; diameter of pads is 22 mil.

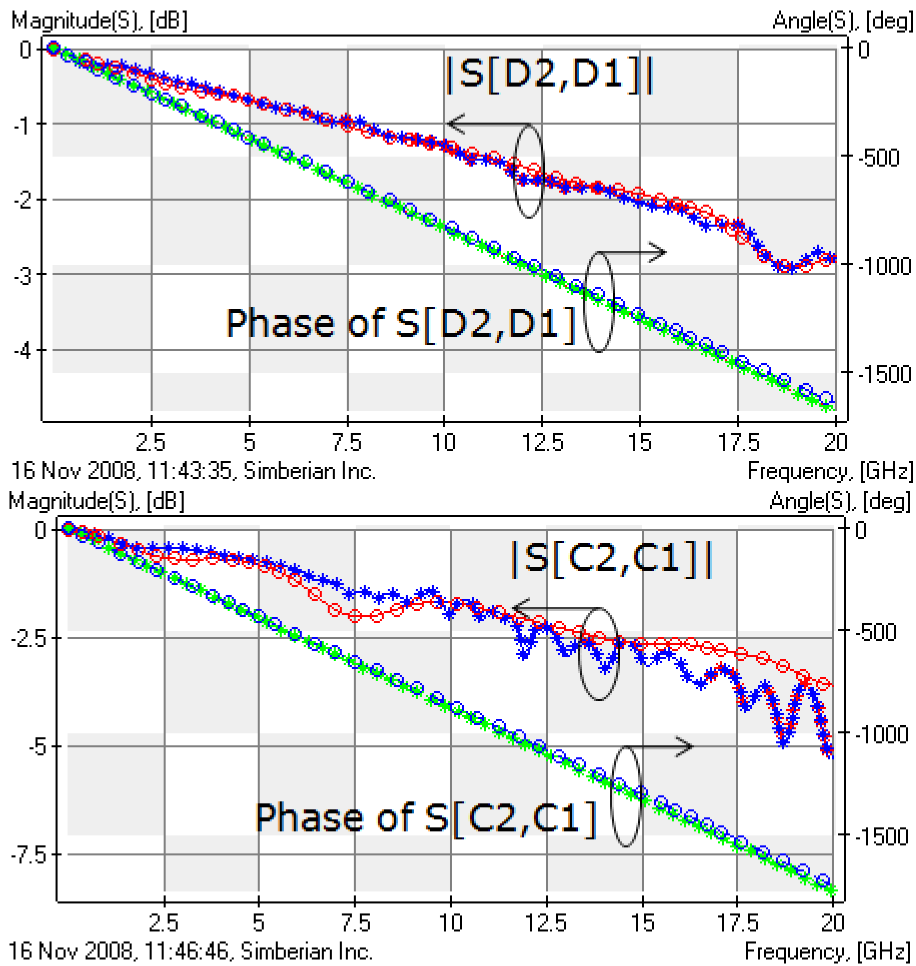

Fig. 7.6. **Differential micro-strip line with differential via-holes:** comparison of measured (stars) and simulated (circles) differential mode transmission coefficients (top graph) and common mode transmission coefficients (bottom graph).

The next structure is a typical micro-strip interconnect with 6 single-ended via-holes with geometry shown in Fig.7.3. Each signal via-holes is isolated with four stitching vias. This is necessary to localize and to reduce the impedance of the current return path, and to make the via-hole behavior predictable with a local electromagnetic analysis. Otherwise, the return path for the via is provided by the parallel planes – the impedance of such transition is large and the transition of high-frequency components of the signal through the structure becomes practically impossible. Analysis of single via-holes without stitching vias can be done with a system-level 2D plane solver, but it has no practical value for transmission of signal in multi-gigabit channels. Note that the via-hole geometry (anti-pads and positions of the stitching vias) was optimized during the board design to provide low reflection. The reflection from the actual via-hole on the board was larger due to wrong original data from manufactured on the dielectric constant. Though the final via geometry is relatively close to optimal and acceptable for practical 6-10 Gb/s data channels as follows from the transmission coefficient magnitude and phase plotted in Fig. 7.4. The resonances in the transmission coefficient are caused by the reflections from via-holes and by multiple line segments with identical length between the via-holes. Note that use of line segments with non-identical lengths can substantially reduce the resonances and improve the transmission quality.

The final structure is differential transmission line with differential via-holes shown in Fig. 7.5. Differential line segments are connected to via-holes on one side and to single-ended micro-strip lines on the other side. This is done to use single-ended de-embedding procedure for the four-port structure. The reference planes of four ports are depicted as RP1-RP4 in Fig. 7.5 and are shifted 250 mil from the differential segments. As in the case of single-ended via-hole, the geometry of the differential vias has been optimized to minimize the reflection of the differential mode. The final via-holes are somewhat sub-optimal due to wrong initial data on the dielectric constant. Though the final via-holes are acceptable for 6-10 Gb/s transmission and the model shows good agreement with the measured data as shown in Fig. 7.6. We can see better correspondence for the differential mode transmission (top graph in Fig. 7.6) and acceptable correspondence in the common mode transmission. Four stitching via-holes are used around the differential via-holes to localize the common mode.

Comparisons for just three structures from the test board are shown here. We observed either good or practically acceptable correspondence for all other structures on the test board that are not covered here. **We can conclude that the suggested material extraction methodology on the base of the frequency-domain measurements and proposed 3D full-wave analysis can be effectively used to predict behavior of high-speed data channels.** All geometry details and measured and simulated S-parameters are available for independent evaluation and benchmarking purpose.

8. Conclusion

The main result of this research is the simulation and measurement methodology to predict behavior of 6-20 Gb/s data channel on a typical low-cost PCBs.
The methodology is based on two key components:

1. Accurate de-embedded S-parameters of resonators or line segments

2. Accurate 3D full-wave electromagnetic analysis with wideband Debye dielectric model and with all conductor-related and high-frequency loss and dispersion effects included

It is observed that the use of resonant structures in t-lines is preferable way to identify dielectric properties due to less sensitivity to de-embedding errors and to connector launches differences. It is shown that behavior of interconnects on low-cost PCBs can be reliably predicted by electromagnetic analysis with the identified material properties. The results of measurements and simulations are available for benchmarking of signal integrity and electromagnetic tools. As the next step, we are planning to develop a practical methodology to identify conductor parameters including roughness, solder mask and core dielectric parameters.

9. References

1. N. K. Das, S. M. Voda, and D. M. Pozar, "Two methods for the measurement of substrate dielectric constant," *IEEE Trans. Microw. Theory Tech.*, vol. MTT-35, N 7, 1987, p. 636-642.
2. D. Shimin, "A new method for measuring dielectric constant using the resonant frequency of a patch antenna," *IEEE Trans. Microw. Theory Tech.*, vol. MTT-34, N 9, 1986, pp. 923–931.
3. P. A. Bernard and J. M. Gautray, "Measurement of dielectric constant using a microstrip ring resonator," *IEEE Trans. Microw. Theory Tech.*, vol. 39, N 3, 1991, p. 592–595.
4. M.-Q. Lee and S. Nam, "An accurate broadband measurement of substrate dielectric constant," *IEEE Microw. Guided Wave Lett*, vol. 6, N 4, 1996, p. 168–170.
5. H. Yue, K. L. Virga, and J. L. Prince, "Dielectric constant and loss tangent measurement using a stripline fixture," *IEEE Trans. Compon., Packag., Manuf. Technol.*, vol. 21, N 11, 1998, p. 441–446.
6. J. Baker-Jarvis, M. Janezic, B. Riddle, C. Holloway, N. Paulter, J. Blendell, Dielectric and conductor-loss characterization and measurements on electronic packaging materials, - *National Institute of Standards (NIST) Technical Note 1520*, July, 2001.
7. A.R. Djordjevic, R.M. Biljic, V.D. Likar-Smiljanic, T.K.Sarkar, Wideband frequency domain characterization of FR-4 and time-domain causality, *IEEE Trans. on EMC*, vol. 43, N4, 2001, p. 662-667.
8. Deutsch, T. Winkel, G. Kopcsay, C. Surovic, Extraction of eps(f) and tand(f) for printed circuit board insulators up to 30 GHz using the short-pulse propagation technique, – *IEEE Trans. on Adv. Packaging*, v. 28 N 1, 2005, p. 4-12.
9. E.L. Holtzman, Wideband measurement of the dielectric constant of an FR4 substrate using a parallel-coupled microstrip resonator, *IEEE Trans. on MTT*, v. 54, N7, 2006, p. 3127-3130.
10. J. Zhang, J.L. Drewniak, D.J. Pommerenke, R.E. DuBroff, Z. Yang, W. Cheng, J. Fisher, S. Camerlo, Signal link-path characterization up to 20 GHz based on a stripline structure, - *in Proc. of EMC Symposium*, 2006.

11. D.-H. Han, M.J. Choi, J. Suk, W.H. Ryu, Frequency-dependent physical-statistical material property extraction for tabular W-element model based on VNA measurements, - *in Proc. of DesignCon2006*.
12. E. Engin, A. Tambawala, M. Swaminathan, S. Bhattacharya, P. Pramanik, K. Yamazaki, Dielectric constant and loss tangent characterization of thin high-K dielectric using corner-to-corner plane probing, - *in Proc. of EPEP 2006*, p. 29-32.
13. B.O. McCoy, B.R. Buhrow, B.K. Gilbert, E.S. Daniel, Broadband resonant-plate permittivity measurement technique for printed wiring boards aided by electromagnetic simulations – *in Proc. of DesignCon2008*.
14. C. Morgan, Solutions for causal modeling and a technique for measuring causal, broadband dielectric properties – *in Proc. of DesignCon2008*.
15. J. Zhang, M.Y. Koledintseva, J.L. Drewniak, D.J. Pommerenke, R.E. DuBroff, Z. Yang, W. Cheng, R.N. Rozanov, C. Antonini, A. Orlandi, Reconstruction of dispersive dielectric properties for PCB substrates using genetic algorithm, - *IEEE Trans. on EMC*, vol. 50, N 3, 2008, p. 704-714.
16. W. Kim, J.H. Kim, D. Oh, C. Yuan, Implementation of broadband transmission line models with accurate low-frequency response for high-speed system simulations, - *in Proc. of DesignCon2006*.
17. H. Shi, G. Liu, A. Liu, Accurate calibration and measurement of non-insertable fixtures in FPGA and ASIC device characterization, - *in Proc. of DesignCon2006*.
18. I. Novak, J.R. Miller, *Frequency Domain Characterization of Power Distribution Networks,* Artech House, 2007, Chapter 4.
19. C. Svensson, G.E. Dermer, Time domain modeling of lossy interconnects, IEEE Trans. on Advanced Packaging, May 2001, N2, Vol. 24, pp.191-196.
20. G. Kron, Diakoptics, Macdonald, London, 1963.
21. V.V. Nikol'skii, T.I. Nikol'skaia, *Decompositional approach to electromagnetic problems*. Moscow: Nauka, 1983 (in Russian).
22. R. Pregla, W. Pascher, "The method of lines", in *Numerical techniques for microwave and millimeter-wave passive structures*, Edited by T. Itoh, J. Willey Publ., New York, 1989, p. 381-446.
23. Y.O. Shlepnev, Extension of the Method of Lines for planar 3D structures - *in Proceedings of the 15th Annual Review of Progress in Applied Computational Electromagnetics (ACES'99)*, Monterey, CA, 1999, p.116-121.
24. Y. O. Shlepnev, B.V. Sestroretzkiy, V.Y. Kustov, A new approach to modeling arbitrary transmission lines. - *Journal of Communications Technology and Electronics*, v. 42, 1997, N 1, p. 13-16.
25. J.C. Rautio, A new definition of characteristic impedance, *IEEE MTT-S Int. Microwave Symp. Digest*, 1991, p.761-764.
26. A.P. Goswami, *Implementation of Microwave Measurements Using Novel Calibration Techniques*, Masters Thesis, NC State University, May 2003
27. Simbeor 2008 Electromagnetic Software, Simberian Inc., www.simberian.com
28. ADS2008 Software, Agilent Technologies, http://eesof.tm.agilent.com/